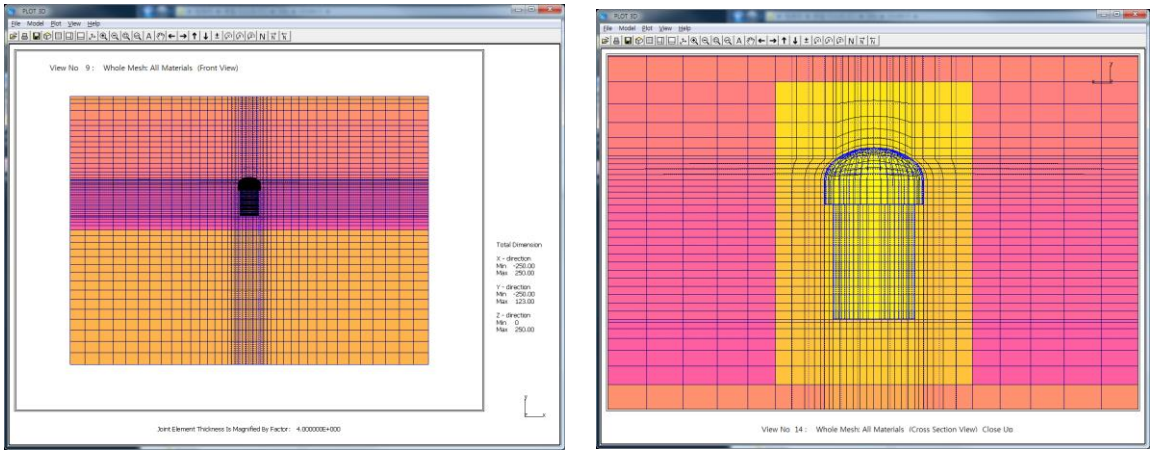

(a) Whole 2-D finite element mesh (b) FE model before silo excavation

Fig. 3 2-D Axi-symmetric Finite Element Model of Silo Type Underground Cavern

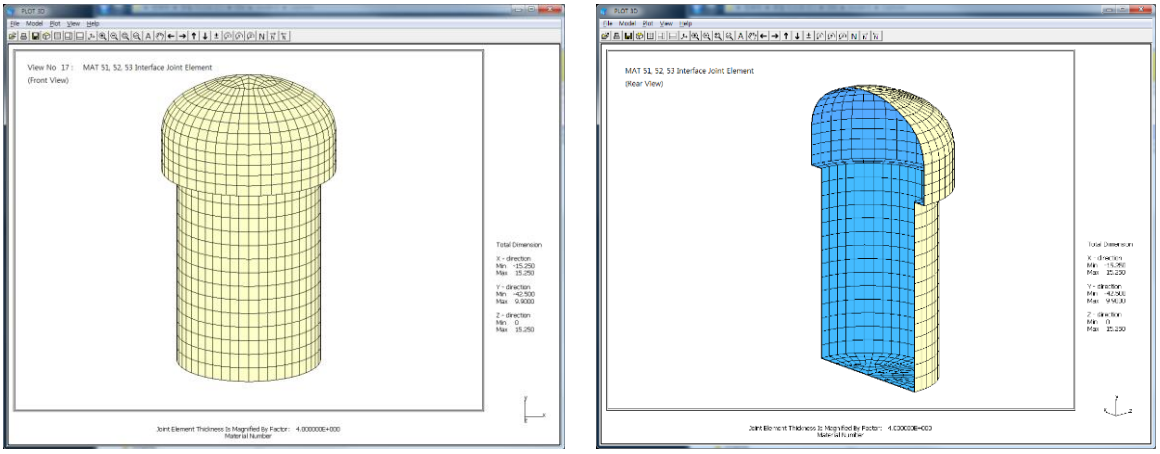

Fig. 4 3-D Finite Element Model of Silo Type Underground Cavern

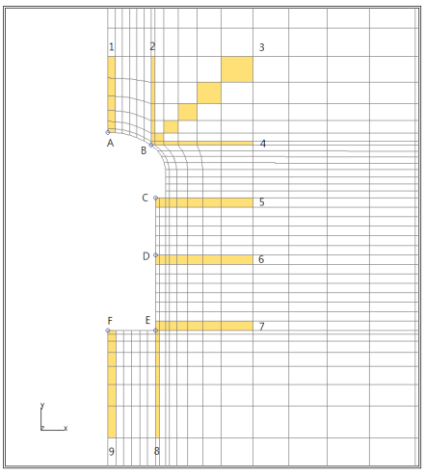

Fig. 5 Key Locations of Finite Element Model

4. NUMERICAL RESULTS

The numerical results of 2-D axis symmetric excavation analysis were almost identical to them of 3-D excavation analysis as shown in Table 2. The deformed shape according to change in the ratio of average horizontal stress and vertical stress (Ko) after excavation of silo type underground cavern are shown in Fig. 6. The displacements at key locations according to change in the ratio of average horizontal stress and vertical stress (Ko) are also compared in Table 3.

Table 2. Comparison of Displacements Between 2D and 3D Analyses

Locations (Node)	Displacement (mm)	Ko = 0.5	Ko = 1.0	Ko = 2.0
A (36)	Radial	0.0	0.0	0.0
	Vertical	-0.489 (-0.485)	-0.379 (-0.375)	-0.158 (-0.153)
B (46)	Radial	-0.078 (-0.076)	-0.234 (-0.230)	-0.547 (-0.538)
	Vertical	-0.321 (-0.318)	-0.235 (-0.234)	-0.064 (-0.064)
C (85)	Radial	-0.209 (-0.208)	-0.542 (-0.540)	-1.208 (-1.205)
	Vertical	0.286 (0.284)	0.285 (0.284)	0.283 (0.283)
D (167)	Radial	-0.319 (-0.318)	-0.652 (-0.651)	-1.320 (-1.316)
	Vertical	0.087 (0.087)	0.070 (0.070)	0.037 (0.038)
E (191)	Radial	-0.067 (-0.067)	-0.191 (-0.191)	-0.439 (-0.438)
	Vertical	0.282 (0.281)	0.206 (0.206)	0.054 (0.055)
F (107)	Radial	0.0	0.0	0.0
	Vertical	0.850 (0.848)	0.786 (0.785)	0.659 (0.658)

Note: 3D results are in ()

.

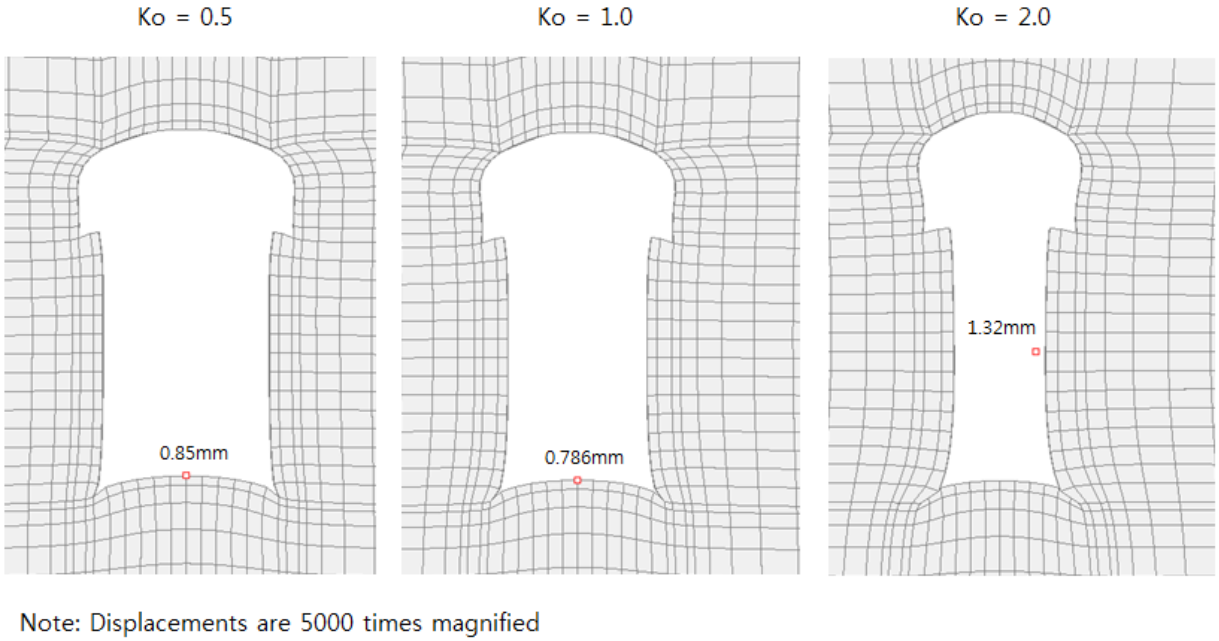

Fig. 6 Deformed Shape after Excavation

Table 3. Displacements at Key Locations

Locations (Node)	Displacement (mm)	Ko = 0.5	Ko = 1.0	Ko = 2.0
A (36)	Radial	0.0	0.0	0.0
	Vertical	-0.489	-0.379	-0.158
B (46)	Radial	-0.078	-0.234	-0.547
	Vertical	-0.321	-0.235	-0.064
C (85)	Radial	-0.209	-0.542	-1.208
	Vertical	0.286	0.285	0.283
D (167)	Radial	-0.319	-0.652	-1.320 (Max)
	Vertical	0.087	0.703	0.037
E (191)	Radial	-0.067	-0.191	-0.439
	Vertical	0.282	0.206	0.054
F (107)	Radial	0.0	0.0	0.0
	Vertical	0.850 (Max)	0.786 (Max)	0.659

The relationship between mean pressure and deviatoric stress (Hoek and Brown 1984) at key locations according to change in the ratio of average horizontal stress and vertical stress (Ko) are shown in Fig. 7~9. In the case of Ko=1.0, the results close to the Mohr-Coulomb tension mode line at C5 were shown in Fig. 8(a). In the case of Ko=2.0, the results close to the Mohr-Coulomb compression mode line as well as beyond the Mohr-Coulomb tension mode line were shown in several regions near the cylindrical space as shown in Fig. 9.

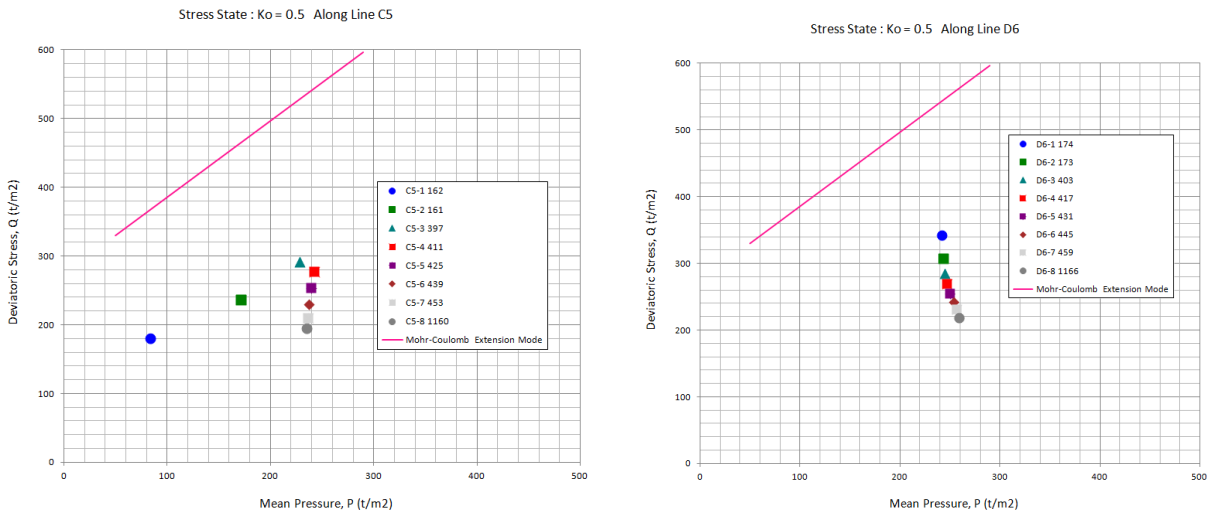

(a) Line C5 (b) Line D6

Fig. 7 Stress State along the Line C5 and D6 (Ko=0.5)

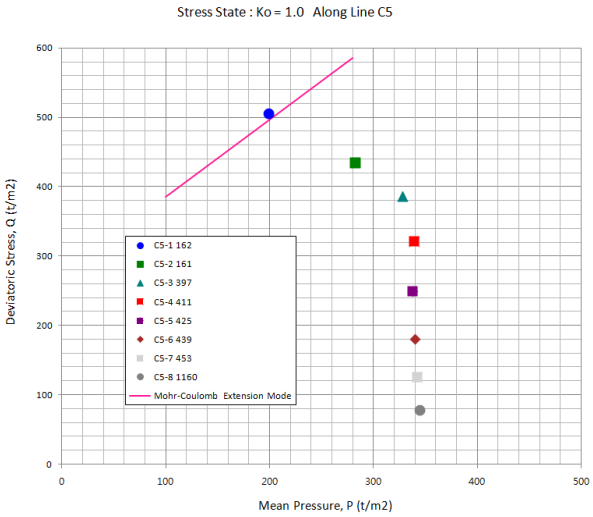

(a) Line C5

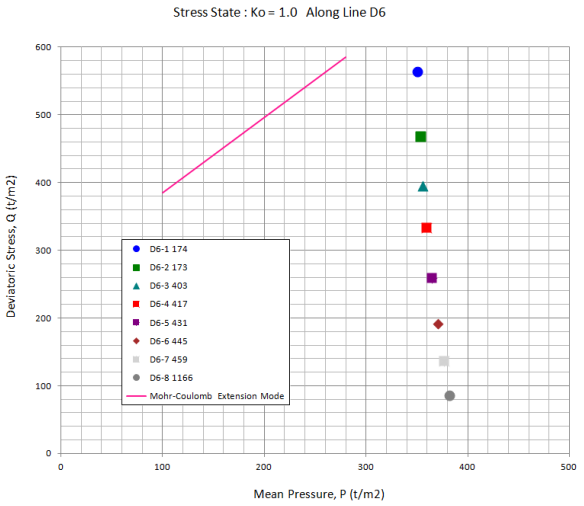

(b) Line D6

Fig. 8 Stress State along the Line C5 and D6 (Ko=1.0)

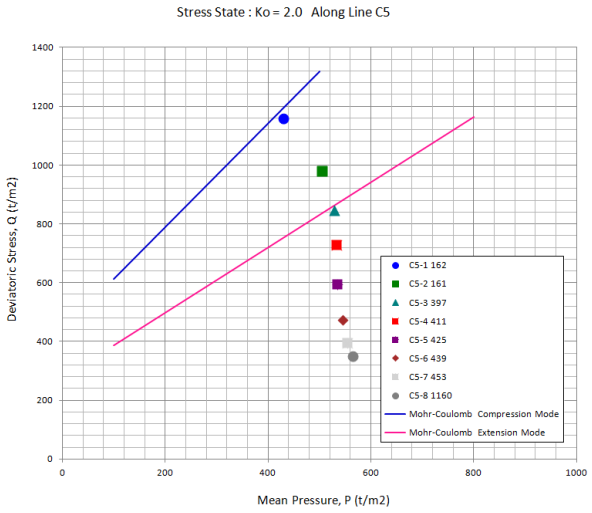

(a) Line C5

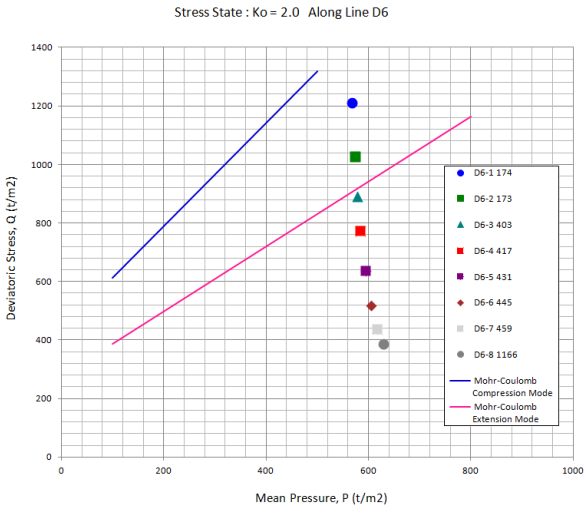

(b) Line D6

Fig. 9 Stress State along the Line C5 and D6 (Ko=2.0)

5. CONCLUSIONS

Finite element analysis of the silo type underground cavern for LILW (Low- and Intermediate-Level radioactive waste) disposal facilities in Korea is carried out. The 3-D finite element model as well as 2-D axial symmetric finite element model are considered

in this study. The excavation analysis of the silo type underground cavern is also performed under various ratios of horizontal stress and vertical stress, and numerical results of these analyses are presented. The numerical results of 2-D axis symmetric excavation analysis were almost identical to them of 3-D excavation analysis. In the case of Ko=2.0, the relationship between mean pressure and deviatoric stress close to the Mohr-Coulomb compression mode were shown in some area near the cylindrical space.

ACKNOWLEDGEMENT

This work was partially supported by the “Radioactive Waste Management Program” of the Korea Institute of Energy Technology Evaluation and Planning (KETEP) granted financial resources from the Ministry of Trade, Industry and Energy, Republic of Korea (Project No. 20193210100040).

REFERENCES

Comtec Research (2020), “SMAP-3D; Structure Medium Analysis Program,” User’s Manual Version 7.03.

Ha, J.C. (2014), “Modeling Approach for Environmental Changes inside the Silo in Low- and Intermediate-Level Radioactive Waste Disposal Facilities,” MS Thesis, Chungnam National University

Hoek, E. and Brown, E.T. (1984), Underground Excavations in Rock, The Institution of Mining and Metallurgy: London.

Kim, M.K., Choi, I.K. and Jeong, J. (2011), “Development of a Seismic Risk Assessment System for Low and Intermediate Level Radioactive Waste Repository – Current Status of Year 1 Research,” WM2011 Conference, Phoenix, AZ.

Kim, S.H. and Kim, K.J. (2000), “Two-phase Finite Element Procedures for Dynamic Analysis of Saturated Porous Media,” Engineering Computations, **17**(7), 758-774.

Kim, S.H. and Kim, K.J. (2001), “Three-dimensional Dynamic Response of Underground Openings in Saturated Rock Masses,” Earthquake Engineering and Structural Dynamics, **30**, 765-782.

KORAD (2018), Earth & Us, Korea Radioactive Waste Agency.

Nawel, B. and Salah, M. (2015), “Numerical modeling of two parallel tunnels interaction using three-dimensional Finite Elements Method,” Geomechanics and Engineering, **9**(6), 775-791.

Park, J.B. et al. (2009), “Wolsong Low- and Intermediate-Level Radioactive Waste Disposal Center: Progress and Challenges,” Nuclear Engineering and Technology, **41**(4), 477-492.

Shin, Y. and Lee, J. (2017), “The Status and Experiences of LILW Disposal Facilities Construction,” J. Korean Soc. Miner. Energy Resour. Eng., **54**(4), 389-396.